MITSUBISHI ELECTRIC RESEARCH LABORATORIES
https://www.merl.com

Robust 3D Tomographic Imaging of the Ionospheric Electron Density

Xu, Xiaojian; Dhifallah, Oussama; Mansour, Hassan; Boufounos, Petros T.; Orlik, Philip V.

TR2020-113 July 22, 2020

Abstract

In this paper, we develop a robust three dimensional tomographic imaging framework to estimate the ionospheric electron density using ground-based total electron content (TEC) measurements from GPS receivers. In order to increase the sampling rate of the domain, we incorporate into the tomographic measurements the TEC readings observed from low-angle satellites that fall outside of the target ionospheric domain. We discount the proportion of the TEC measurements that originate outside of the target domain using the simulation-based NeQuick2 model as reference. We also employ a diffusion kernel regularization function to robustify the reconstruction against errors in the NeQuick2 model. Finally, we demonstrate through simulations that our framework delivers superior reconstruction of the ionospheric electron density compared to existing schemes. We also demonstrate the applicability of our approach on real TEC measurements.

IEEE International Geoscience and Remote Sensing Symposium (IGARSS)

Mitsubishi Electric Research Laboratories, Inc.
201 Broadway, Cambridge, Massachusetts 02139

ROBUST 3D TOMOGRAPHIC IMAGING OF THE IONOSPHERIC ELECTRON DENSITY

Xiaojian Xu[1*], *Oussama Dhifallah*[2†], *Hassan Mansour*[3], *Petros T. Boufounos*[3], *Philip V. Orlik*[3]

[1]Computer Science and Engineering, Washington University in St. Louis, St. Louis, MO 63130
[2]John Paulson School of Engineering and Applied Science, Harvard University, Cambridge, MA 02138
[3]Mitsubishi Electric Research Laboratories, Cambridge, MA 02139
xiaojianxu@wustl.edu; oussama_dhifallah@g.harvard.edu; {mansour, petrosb, porlik}@merl.com

ABSTRACT

In this paper, we develop a robust three dimensional tomographic imaging framework to estimate the ionospheric electron density using ground-based total electron content (TEC) measurements from GPS receivers. In order to increase the sampling rate of the domain, we incorporate into the tomographic measurements the TEC readings observed from low-angle satellites that fall outside of the target ionospheric domain. We discount the proportion of the TEC measurements that originate outside of the target domain using the simulation-based NeQuick2 model as reference. We also employ a diffusion kernel regularization function to robustify the reconstruction against errors in the NeQuick2 model. Finally, we demonstrate through simulations that our framework delivers superior reconstruction of the ionospheric electron density compared to existing schemes. We also demonstrate the applicability of our approach on real TEC measurements.

Index Terms— Ionosphere Mapping, GPS, Tomographic Imaging, Total Electron Content

1. INTRODUCTION

The ionosphere is the ionized region of the Earth's atmosphere spanning the altitudes between 60km to 1000km above the Earth's surface. Electrons are distributed in the ionosphere and act as a transportation medium as well as an interference channel for electromagnetic signals that are utilized by the global positioning system (GPS). Therefore the inference of the ionospheric electron density distribution has long been a focus of ionospheric study.

Computerized Ionospheric Tomography (CIT) from total electron content (TEC) measurements along line-of-sight (LOS) from the naval navigational satellite system (NNSS) to ground-based receivers was first proposed in [1, 2]. Every TEC measurement constitutes an accumulation along the LOS, or line integral, across the electron density volume. As such, a given LOS ray indexed by i can be written as

$$\text{TEC}_i = \int_{rec}^{sat} N_e(\rho) d\rho, \tag{1}$$

where $N_e(\rho)$ denotes the electron density along the LOS connecting the receiver rec and the satellite sat. By dividing the three-dimensional space into small grids, we can discretize the observation model as follows:

$$\mathrm{y}_i = \sum_{k=1}^{n} a_{ik} x_k, \tag{2}$$

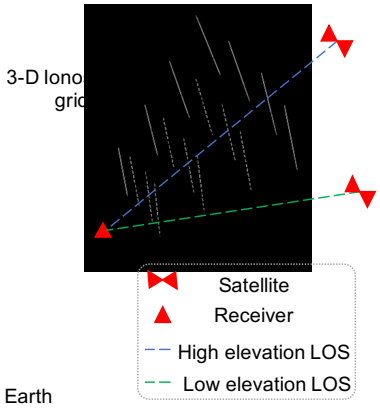

Fig. 1. Illustration of 3-D Ionosphere tomography model with two types of LOS: low elevation path and high elevation path.

where we have renamed the variables such that, y_i denotes the measured TEC at ray i, n is the total number of grid points along the LOS ray, a_{ik} denotes the length of path i in grid k, and x_k denotes the electron density in grid k. Note that in this case, when the LOS ray i does not pass through grid k, a_{ik} is set to zero. The above discretized equation can be written as a linear system of equations

$$\mathbf{y} = \mathbf{A}\mathbf{x}, \tag{3}$$

where $\mathbf{y} \in \mathbb{R}^m$ denotes the 2-D ground based TEC measurements, $\mathbf{A} \in \mathbb{R}^{m \times n}$ denotes the linear forward model, and $\mathbf{x} \in \mathbb{R}^n$ is the vectored ionosphere density distribution that we want to infer.

In this paper, we address the realistic scenario where TEC measurements are acquired from both high elevation and low elevation paths. Figure 1 illustrates such an acquisition scenario with an example of a high elevation path connecting to a satellite located within the target domain and a low elevation path connected to a satellite located outside of the target domain. Inclusion of the low elevation paths is important for increasing the density of the rays passing through the target domain. Notice that the TEC measurement from the low elevation path includes electrons that are located outside of the domain. To address this problem, we adopt a TEC correction strategy that discounts the low elevation TEC measurement by an amount proportional to that estimated by the NeQuick2 model [3]. Since the NeQuick2 model may differ from the true electron density distribution, we employ domain regularization using a diffusion kernel penalty function to robustify the reconstruction to measurement mismatch.

*X. Xu contributed to this work during an internship at MERL.
†O. Dhifallah contributed to this work during an internship at MERL.

In Section 2 we review previous work on 3D tomographic imaging. We then describe in Section 3 the TEC acquisition setup and present our robust 3D tomographic imaging formulation. In Section 4 we present numerical simulations that demonstrate that our proposed framework outperforms existing methods.

2. PRIOR WORK

Computerized ionospheric tomography has received significant attention in the literation. Some CIT methods require a background initial value of the ionospheric volume which is then corrected using variations of the algebraic reconstruction technique [4, 5]. Seemala et al. [6] proposed a constrained least square method without model-based initialization which utilized constraint parameters that are empirical and model-based. Chen et al. [7] follow a similar approach with model-free diffusion kernel constraint. In [8], a neural network architecture is used to reconstruct the 3D electron density using GPS-TEC and ionosonde data, giving an effective estimation of vertical profile. However, none of the above works take advantage of the low elevation LOS paths, which are in fact the majority of the measurements. In [9], low elevation paths are incorporated by means of an NeQuick2-based TEC discounting procedure and a modification of SIRT algorithm is utilized for reconstruction. However, the approach in [9] cannot overcome the model mismatch that comes from inaccurate NeQuick2 modeling. Therefore, we develop in this study a methodology using all elevation TEC measurements, including low elevation ones that only partially intersects with our ROI. We show with the experiments that such comprehensive TEC measurements will greatly improve our reconstruction accuracy.

3. ROBUST 3D IONOSPHERIC TOMOGRAPHY

In this section, we present TEC acquisition from the raw GPS data and then discuss our proposed reconstruction method.

3.1. Computation of TEC from GPS data

There are 28 GNSS satellites currently orbiting the Earth at a height of 20200 km broadcasting information on two carrier frequencies via RINEX message files. These two radio signals are delayed by different amount and based on these delays, two known ways to compute TEC are derived [10]based on the pesudo-ranges P_1 and P_2 (referred as TEC$_{pr}$), and on the carrier phase L_1 and L_2 (referred as TEC$_{cp}$):

$$\text{TEC}_{pr} = \frac{2}{k}\frac{f_1^2 f_2^2}{f_1^2 - f_2^2}(P_2 - P_1), \tag{4}$$

$$\text{TEC}_{cp} = \frac{2c}{k}\frac{f_1^2 f_2^2}{f_1^2 - f_2^2}(L_1/f_1 - L_2/f_2). \tag{5}$$

Note here $k = 80.62(m^3/s^2)$ is the ionosphere refraction, c is the speed of light, and $f_1 = 1.57542$GHz, $f_2 = 1.2276$GHz are two frequencies satellites transmit on. However, the TEC$_{pr}$ estimate is very noisy and the TEC$_{cp}$ is less noisy but suffers from cycle slips. In this work, we follow the approach of [11] and compute the GPS slant TEC (sTEC) by combining TEC$_{cp}$ and TEC$_{pr}$ together. A series of refining operations were also done to remove the ambiguity and correct the cycle slips, estimate the instrument biases, smooth the vertical TEC (vTEC). We leave the details to [11] due to the page limitation.

The GPS-TEC measurement we compute above is an accumulation of the electron density along the complete LOS path. To compensate for the counted electrons that lie outside of the target region of interest (ROI), we follow an approach similar to [9] and assume that the GPS-TEC inside the ROI along a LOS is proportional to the TEC inside the ROI of the ionospheric density estimated by the NeQuick model. Specifically, for all LOS paths l belonging to the set of low elevation paths $\mathcal{L}$, we compute the correction

$$\tilde{y}_l = y_l \left(\frac{\text{partial TEC}_{l,\text{NeQuick}}}{\text{TEC}_{l,\text{NeQuick}}}\right)^p, \ \forall\, l \in \mathcal{L} \tag{6}$$

where $\tilde{y}_l$ is the corrected partial TEC, y_l is the total slant GPS-TEC, and p is an exponent that is used to scale the discount level of the partial TEC measurements. Note that since the NeQuick model may differ from the true electron density distribution, the TEC discounting strategy used above could cause model mismatch. We address this problem using a penalty function regularization as will be discussed in the next section.

3.2. Reconstruction method

We formulate the problem of reconstructing the ionospheric volume as the following regularized least squares problem:

$$\begin{aligned}\widehat{\mathbf{x}} = \underset{\mathbf{x}\in\mathbb{R}^n}{\arg\min}\ & \|\mathbf{y} - \mathbf{A}\mathbf{x}\|_2^2 + \lambda\|\mathbf{W}\mathbf{x}\|_2^2 + \gamma\sum_{q=1}^{h}\|\mathbf{R}_q\mathbf{x} - \mathbf{x}_q\|_2^2 \\ \text{s.t.}\quad & \mathbf{x} \geq 0,\end{aligned} \tag{7}$$

where $\mathbf{y}$ are the TEC measurements computed as in Section 3.1, $\mathbf{A}$ is the forward model computed by the ray tracing method [12], $\mathbf{x}_q$ and $\mathbf{R}_q$ are reference electron density profiles and their respective restriction operator that can be extracted from ionosonde[1] or COSMIC[2] measurements, $\lambda \geq 0$ and $\gamma \geq 0$ are regularization parameters, and $\mathbf{W} \in \mathbb{R}^{n\times n}$ is a weighted diffusion kernel matrix that denotes the coupling of the ionosphere density in grid i and its six neighbors

$$(\mathbf{W}\mathbf{x})_i = \sum_{k=1}^{6} C_{ik}(x_i - x_{ik}). \tag{8}$$

Note here $C_{ik} \geq 0$ is a parameter that indicates the weighting of the neighboring gridpoint ik. The constraint parameter C_{ik} could either be fixed for all grid points, or it could chosen such that a smaller value is set in the mid-altitude regions where the electron density encounters fast changes or a larger value is set in the boundary regions where the electron density is generally smooth. Inspired by [7], we define adaptive constraint parameters C_i at gird i as a function of the latitude, longitude, and altitude based on the empirical electron density model NeQuick:

$$C_i = \frac{(1 - \text{vTEC}^i_{\text{NeQuick}}/(\text{vTEC}^{i(max)}_{\text{NeQuick}} + R))^{1.2}}{10}. \tag{9}$$

Here vTEC$^i_{\text{NeQuick}}$ denotes the NeQuick vertical TEC at a grid i, vTEC$^{i(max)}_{\text{NeQuick}}$ is the maximum density distribution at the latitude and longitude of grid i , and $R = 1.0 \times 10^{11}(el/m^3)$ is an adjustment constant.

To solve (7), we use Nesterov's accelerated gradient descent [13] technique which enjoys a low computational complexity and fast convergence rate.

[1] https://data.ngdc.noaa.gov/instruments/remote-sensing/active/profilers-sounders/ionosonde/

[2] http://cdaac-www.cosmic.ucar.edu/

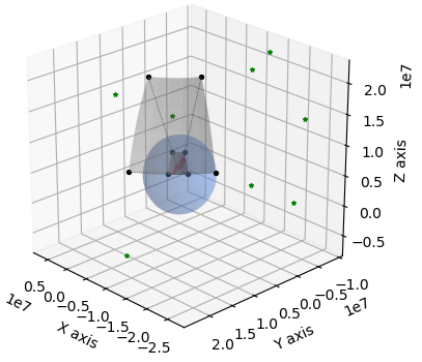

Fig. 2. Illustration of the observed satellites and GPS ground stations in the region above Japan at 13:30 UT on May 17, 2019. The gray shaded region illustrates the reconstruction volume.

4. NUMERICAL RESULTS

In the following experiments, we focus on the reconstruction of 3-D ionosphere density model in the region above Japan at 13:30 UT on May 17, 2019. We downloaded the data from 500 GPS ground stations provided by the Geospatial Information Authority of Japan website[3], and we ignore the vertical TEC reference profiles in the reconstruction, i.e., we set $\gamma = 0$ in (7) for fairness of comparison with [9]. From the 500 GPS ground stations, we observe 3314 slant TEC measurements of which 98% are partial TEC measurements that have been discounted using the corresponding NeQuick model for that date and time. Figure 2 illustrates the observed satellites and ground stations. Notice that out of eight visible satellites, seven satellites produce partial TEC measurements. The 3D ionospheric volume spans an elevation from 80 to 20000 km with a latitudinal range is $22^\circ N$ to $56^\circ N$ and the longitudinal range is $118^\circ E$ to $178^\circ E$. The grid was discretized to 1° in the latitudinal and longitudinal dimensions and using a variable elevation resolution ranging from 20 km for low elevations to 5000 km for high elevations. To measure the accuracy of our reconstruction, we use the relative error:

$$\text{relative error} = \|\widehat{\mathbf{x}} - \mathbf{x}^*\|_2 / \|\mathbf{x}^*\|_2, \tag{10}$$

where $\widehat{\mathbf{x}}$ is the reconstruction result and $\mathbf{x}^*$ is the ground truth.

To demonstrate the accuracy of our reconstruction method, we first conduct simulation-based experiments using the NeQuick model as ground truth. We construct the forward operator $\mathbf{A}$ corresponding to the date and time described above and synthesize the slant TEC measurements by multiplying $\mathbf{A}$ with $\mathbf{x}^*$. We compare the performance of our method with that of the modified SIRT [9]. For both methods, we use an initial estimate of the electron density as the ground truth $\mathbf{x}^*$ with 20% additive white Gaussian noise. Figure [**?**] illustrates the reconstruction performance of both methods. Our propose approach achieves a reconstruction relative error of 9.76×10^{-2} compared to 1.92×10^{-1} for modified SIRT and 2×10^{-1} for the initial estimate.

Next, we test the robustness of both techniques to model mismatch by varying the accuracy of the discounting factor in the partial TEC computation. Considering the same setup as above, we modify the partial TEC measurements by setting the exponent p in 6 equal to 1, 2, and 4. Table 1 summarizes the reconstruction results as a function of p. The table demonstrates that our proposed approach remains robust to model mismatch, whereas modified SIRT is more seriously affected by the measurement error.

Table 1. Relative error (RE) sensitivity to mismatch in partial TEC

Exponent p in (6)	Proposed RE	modified SIRT RE
1	0.0976	0.192
2	0.104	0.197
4	0.133	0.215

Finally, we compare the recovery performance of the proposed method to the electron density profile generated by the COSMIC low earth orbit mission that collects electron density observations in addition to atmospheric monitoring. We set the initial model to be a scaled down version of the NeQuick model with 5% additive white Gaussian noise. Figure 4 shows the reconstructed vertical electron density profiles generated by the proposed method, compared to the modified SIRT reconstruction, the NeQuick model, the initial model, and the COSMIC profile. It can be seen that our proposed model results in the closest match to the COSMIC model. This is particularly true of the peak density estimation around the 350km altitude which is most essential for timing corrections. We also observe a relatively large bias in our reconstruction especially in the lower altitudes which results from the diffusion kernel regularization. This bias is not observed in the initial estimate or the modified SIRT reconstruction since the modified SIRT does not seem to result in vast deviations from the initial model.

5. CONCLUSION

In this study, we proposed a robust 3D tomographic imaging technique that can recover from model mismatch. The model mismatch setting arises especially when slant TEC measurements are acquired from low elevation line of sight paths. We showed with simulation and real data experiments that our approach improves the reconstruction performance of ionospheric tomography compared to the recently proposed modified SIRT approach of [9].

6. REFERENCES

[1] J.R. Austen, S.J. Franke, CH Liu, and KC Yeh, "Application of computerized tomography techniques to ionospheric research," in *International Beacon Satellite Symposium*, 1986, pp. 25–35.

[2] Jeffrey R Austen, Steven J Franke, and CH Liu, "Ionospheric imaging using computerized tomography," *Radio Science*, vol. 23, no. 3, pp. 299–307, 1988.

[3] B. Nava, P. Coisson, and S.M. Radicella, "A new version f the nequick ionosphere electron density model," *Journal of Atmospheric and Solar-Terrestrial Physics*, 2008.

[4] TD Raymund, "Comparison of several ionospheric tomography algorithms," *Ann. Geophys.*, vol. 13, pp. 1254–1262, 1995.

[5] Dieter Bilitza and Bodo W Reinisch, "International reference ionosphere 2007: Improvements and new parameters," *Advances in space research*, vol. 42, no. 4, pp. 599–609, 2008.

[6] Gopi K Seemala, Mamoru Yamamoto, Akinori Saito, and Chia-Hung Chen, "Three-dimensional gps ionospheric tomography over japan using constrained least squares," *Journal of Geophysical Research: Space Physics*, vol. 119, no. 4, pp. 3044–3052, 2014.

[7] Chia-Hung Chen, A Saito, Chien-Hung Lin, M Yamamoto, S Suzuki, and Gopi K Seemala, "Medium-scale traveling ionospheric disturbances by three-dimensional ionospheric gps to-

[3] http://datahouse1.gsi.go.jp/terras/terras_english.html

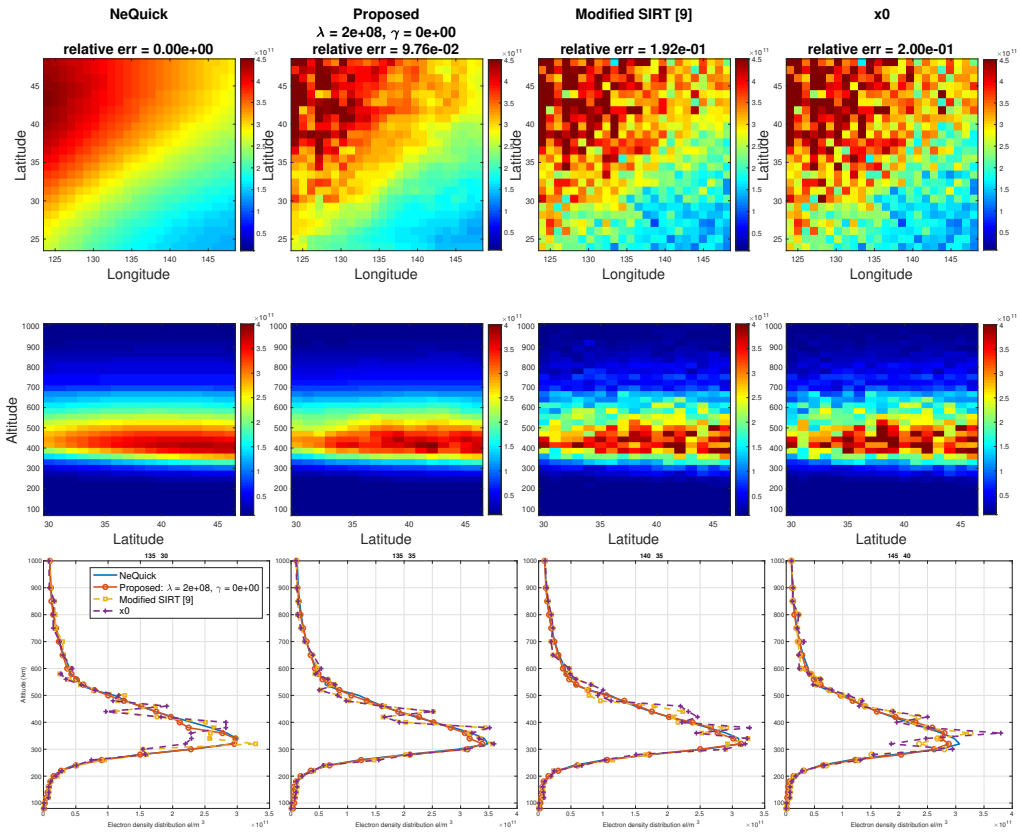

Fig. 3. Comparison of the reconstruction performance from simulated TEC measurements with the modified SIRT method in [9]. The first row show the horizontal slice at elevation 300 km, the second row shows a meridional slice at longitude $135^\circ E$ and the third row shows the vertical profiles at $[135^\circ E, 30^\circ N]$, $[135^\circ E, 35^\circ N]$, $[140^\circ E, 35^\circ N]$. and $[140^\circ E, 40^\circ N]$.

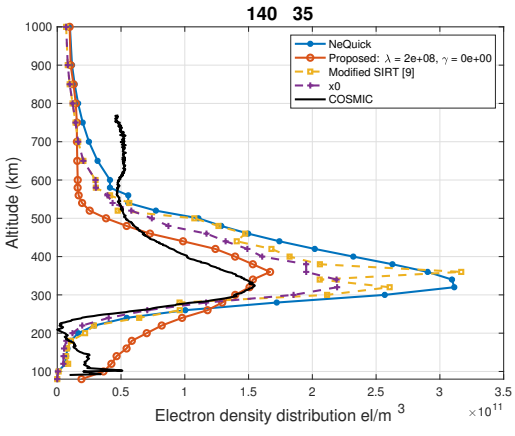

Fig. 4. Comparison of vertical electron density profiles from real data.

mography," *Earth, Planets and Space*, vol. 68, no. 1, pp. 32, 2016.

[8] XF Ma, T Maruyama, G Ma, and T Takeda, "Three-dimensional ionospheric tomography using observation data of gps ground receivers and ionosonde by neural network," *Journal of Geophysical Research: Space Physics*, vol. 110, no. A5, 2005.

[9] Y. Yao, C. Zhai, J. Kong, Q. Zhao, and C. Zhao, "A modified three-dimensional ionospheric tomography algorithm with side rays," *GPS Solutions*, vol. 22, no. 4, pp. 1521–1886, 2018.

[10] Geoffrey Blewitt, "An automatic editing algorithm for gps data," *Geophysical research letters*, vol. 17, no. 3, pp. 199–202, 1990.

[11] G Ma and T Maruyama, "Derivation of tec and estimation of instrumental biases from geonet in japan," in *Annales Geophysicae*, 2003, vol. 21, pp. 2083–2093.

[12] Fabricio dos Santos Prol and Paulo de Oliveira Camargo, "Review of tomographic reconstruction methods of the ionosphere using gnss," *Revista Brasileira de Geofísica*, vol. 33, no. 3, pp. 445–459, 2015.

[13] Yurii Nesterov, "A method for solving the convex programming problem with convergence rate $O(1/k^2)$," in *Soviet Mathematics Doklady*, 1983, vol. 27, pp. 367–372.